

<b>Report Documentation Page</b>			<i>Form Approved OMB No. 0704-0188</i>					
<p>Public reporting burden for the collection of information is estimated to average 1 hour per response, including the time for reviewing instructions, searching existing data sources, gathering and maintaining the data needed, and completing and reviewing the collection of information. Send comments regarding this burden estimate or any other aspect of this collection of information, including suggestions for reducing this burden, to Washington Headquarters Services, Directorate for Information Operations and Reports, 1215 Jefferson Davis Highway, Suite 1204, Arlington VA 22202-4302. Respondents should be aware that notwithstanding any other provision of law, no person shall be subject to a penalty for failing to comply with a collection of information if it does not display a currently valid OMB control number.</p>								
1. REPORT DATE <b>AUG 2008</b>	2. REPORT TYPE	3. DATES COVERED <b>00-00-2008 to 00-00-2008</b>						
4. TITLE AND SUBTITLE <b>Characteristics of Surface-Normal Fano Filters on Flexible Plastic Substrates</b>			5a. CONTRACT NUMBER					
			5b. GRANT NUMBER					
			5c. PROGRAM ELEMENT NUMBER					
6. AUTHOR(S)			5d. PROJECT NUMBER					
			5e. TASK NUMBER					
			5f. WORK UNIT NUMBER					
7. PERFORMING ORGANIZATION NAME(S) AND ADDRESS(ES) <b>Air Force Research Laboratory, Materials &amp; Manufacturing Directorate, Wright Patterson AFB, OH, 45433</b>			8. PERFORMING ORGANIZATION REPORT NUMBER					
9. SPONSORING/MONITORING AGENCY NAME(S) AND ADDRESS(ES)			10. SPONSOR/MONITOR'S ACRONYM(S)					
			11. SPONSOR/MONITOR'S REPORT NUMBER(S)					
12. DISTRIBUTION/AVAILABILITY STATEMENT <b>Approved for public release; distribution unlimited</b>								
13. SUPPLEMENTARY NOTES <b>See also ADM002137. Proceedings of the 2008 IEEE International Conference on Nanotechnology (8th) Held in Arlington, TX on August 18-21, 2008.</b>								
14. ABSTRACT <b>see report</b>								
15. SUBJECT TERMS								
16. SECURITY CLASSIFICATION OF: <table border="1" style="display: inline-table; vertical-align: middle;"> <tr> <td style="padding: 2px;">a. REPORT <b>unclassified</b></td> <td style="padding: 2px;">b. ABSTRACT <b>unclassified</b></td> <td style="padding: 2px;">c. THIS PAGE <b>unclassified</b></td> </tr> </table>			a. REPORT <b>unclassified</b>	b. ABSTRACT <b>unclassified</b>	c. THIS PAGE <b>unclassified</b>	17. LIMITATION OF ABSTRACT <b>Same as Report (SAR)</b>	18. NUMBER OF PAGES <b>3</b>	19a. NAME OF RESPONSIBLE PERSON
a. REPORT <b>unclassified</b>	b. ABSTRACT <b>unclassified</b>	c. THIS PAGE <b>unclassified</b>						

# Characteristics of Surface-Normal Fano Filters on Flexible Plastic Substrates

Zexuan Qiang<sup>1</sup>, Hongjun Yang<sup>1</sup>, Li Chen<sup>1</sup>, Huiqing Pang<sup>2</sup>, Zhenqiang Ma<sup>2\*</sup>, Weidong Zhou<sup>1\*</sup> and Gail J. Brown<sup>3</sup>

<sup>1</sup>Department of Electrical Engineering, NanoFAB Center, University of Texas at Arlington, TX 76019

<sup>2</sup>Department of Electrical and Computer Engineering, University of Wisconsin-Madison, WI 53706

<sup>3</sup>Air Force Research Laboratory, Materials & Manufacturing Directorate, Wright Patterson AFB, OH 45433

<sup>1\*</sup> [wzhou@uta.edu](mailto:wzhou@uta.edu), <sup>2\*</sup> [mazq@engr.wisc.edu](mailto:mazq@engr.wisc.edu)

**Abstract** - We report here the angular and polarization dependent transmission characteristics of surface-normal optical filters based on Fano resonances on patterned single crystalline silicon nanomembranes (SiNM), which were fabricated and transferred onto transparent PET plastic substrates using a disruptive SiNM wet transfer process. The measured surface-normal and angle-dependent filter transmission results agree well with the design and simulation based on 3D finite-difference time-domain technique.

## I. INTRODUCTION

Ultra-compact and sensitive filters have a wide range of potential applications like optical fiber communication, optical sensor, and millimeter-wave communication systems. Traditional filters based on thin-film technology, especially for wavelength division multiplexing (WDM) applications, often require hundreds or more individual layers, with stringent thickness tolerances for each layer. Photonic crystal slabs (PCS), with in-plane periodic modulation of dielectric constant introduced in a high-index guiding layer, offer one of the most promising nano platforms for large-scale on-chip photonic integration. The out-of-the-plane optical mode coupling is feasible with the Fano or guided resonance effect [1], where these in-plane guided resonances above the lightline are also strongly coupled to out-of-the-plane radiation modes due to phase matching provided by the periodic lattice structure. Therefore, the guided resonances can provide an efficient way to channel light from within the slab to the external environment, and vice versa [2]. In recent years, filters based on Fano resonance [1,2] have attracted great attention. However, works report to date are mainly based on freestanding membranes, which have some limitations in mechanical robustness and thermal management challenges.

Crystalline semiconductor nanomembranes (NMs), which are transferable, stackable, bondable and manufacturable, offer unprecedented opportunities for unique and novel electronic and photonic devices for vertically stacked high density photonic/electronic integration. High quality single crystalline silicon NMs (SiNM) have been transferred onto various foreign substrates, such as glass, plastics, etc., based on a unique wet transfer process, developed by various groups [3,

4]. Very high performance electronics based on transferable Si/SiGe NMs were also reported recently [4].

In this paper, we employ a slightly modified transfer process and first demonstrate a new ultra-compact Fano filters, based on transferred single crystalline SiNMs on glass substrates, and on flexible PET substrates.

In what follows, we describe the designed parameters and schematic of proposed Fano filter. The experimental results are then provided and analyzed in section III, and the conclusions are concluded in the end.

## II. FILTER PARAMETER DESIGN

Aforementioned filter based on 2D PCS is not necessary to require photonic bandgap. We thus apply three-dimensional finite-difference time domain (3D FDTD) technique with periodic boundary condition (PBC) and perfectly matched layer (PML) in the four lateral and vertical directions, respectively. For the target Fano filter wavelength of 1550 nm and fabricated with the target for the 270-nm thick SiNM on an ITO-coated

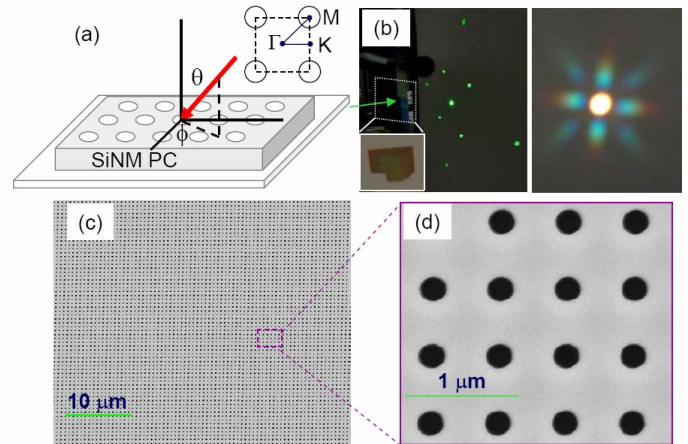


Fig. 1 (a) Schematic of the silicon nanomembranes (SiNMs) transferred onto an ITO-coated PET plastic substrate, with the incident beam direction described with colatitude angle  $\theta$  and azimuth  $\phi$ . The PC lattice and the corresponding directions in K-space ( $\Gamma$ ,  $M$ , and  $K$ ) are also shown in the inset; (b) Measured diffraction patterns through the SiNM on PET sample with either a cw green laser source or a broadband QTH lamp source. The micrograph of the transferred SiNM on PET is shown in the inset (center golden colored piece). (c) and (d) The scanning electron micrographs of patterned SiNMs.

flexible PET plastic substrate, as shown schematically in Fig. 1(a), where the light incident angle are specified by two polar angles, the colatitude angle  $\theta$  (angle from the surface normal direction) and the azimuth angle  $\phi$ , we finally chose those following designed parameters for fabrication, lattice constant of photonic crystal,  $a$  is  $0.6 \mu\text{m}$ , relative hole size,  $r/a$  is 0.19, silicon thickness,  $t/a$  is 0.43, where the indices of silicon and PET substrate in the simulation are assumed as 3.48 and 1.5, respectively. A micrograph of the transferred patterned SiNM on PET is shown in the inset of Fig. 1(b). The scanning electron micrographs (SEMs) of the PC are shown in Figs. 1(c) and 1(d). The high-quality large area uniform pattern was verified also with the diffraction pattern measurement, as shown in Fig. 1(b), where well-defined diffraction patterns were measured with either a cw green laser source (left), or a focused broadband QTH (Quartz-Tungsten-Halogen) lamp source.

### III. EXPERIMENTAL RESULTS AND ANALYSIS

#### A Surface Normal incidence

We first consider a surface normal incidence scenario by using an unpolarized broadband QTH lamp source focused onto a small beam size with an objective lens, where the schematic measurement setup is shown in Fig. 2. Shown in Fig. 3 are our simulated and measured Fano filter transmission characteristics. The experimental results agree well with the design ones, with the target wavelength of  $1.56 \mu\text{m}$ . Another less profound dip can be found around  $1.42 \mu\text{m}$ . Note that further optimization in both design and fabrication can lead to very high Q filters and symmetric spectral responses.

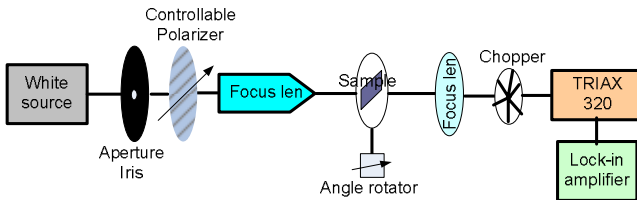


Fig. 2 Schematic of measurement setup where white source here is QTH lamp source

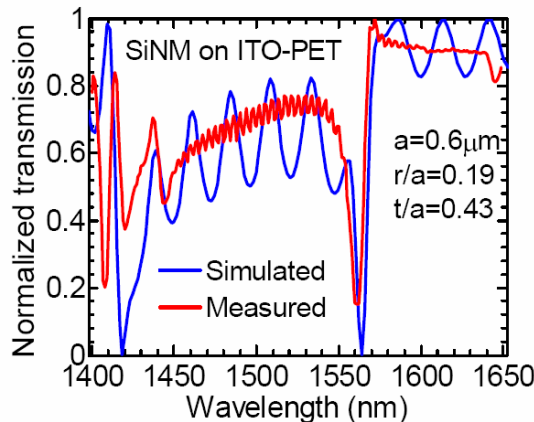
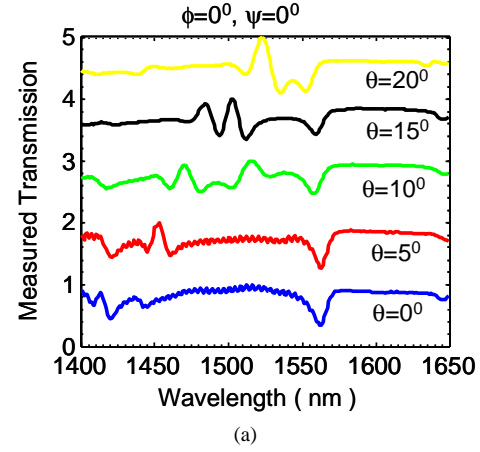


Fig. 3 Measured and simulated surface-normal transmission ( $\theta=0^\circ$ ) characteristics for a patterned SiNM on ITO-coated PET substrate.

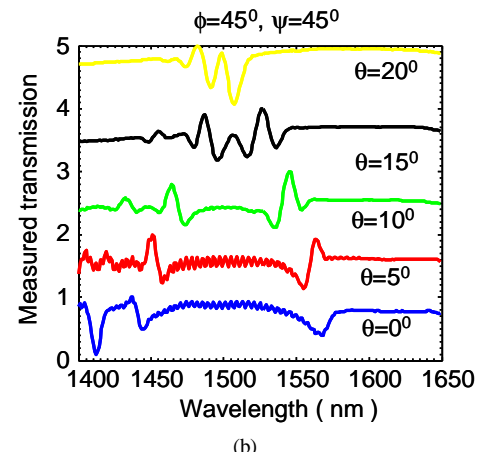
#### B Angle incidence with polarization control

The angle- and polarization-dependent properties are then investigated in more details by controlling the incident beam direction and polarization [5]. Shown in Fig. 4 are two sets of measured transmission spectra for different incident angles  $\theta$ . The colatitude angle  $\theta$  and the azimuth angle  $\phi$  are defined in Fig. 1(a). The incident beam polarization (E-vector)  $\Psi$  is defined as the angle between the polarization direction and PC lattice  $\Gamma\text{X}$  direction (Fig. 1(a)). For the incident beam varying the incident angle  $\theta$  with  $\phi=0^\circ$  and  $\Psi=0^\circ$ , it is very interesting that the dominant mode spectral location around  $1556 \text{ nm}$  remains almost unchanged over the range of angles we measured (from  $0$  to  $20^\circ$ ). At the same time, the other mode (or set of modes) at shorter wavelengths, shift towards longer wavelengths, with the increase of incident angle. The complete measured transmission spectra maps are plotted again in Fig. 5(a), where the vertical blue line corresponds to the  $1556\text{nm}$  dip in the transmission plot shown in Fig. 4(a).

The corresponding simulation results are shown in Fig. 5(c), where the measured transmission peaks/dips are plotted in the dispersion chart for the corresponding incident angles. Very good agreement is obtained.



(a)



(b)

Fig. 4. Measured angle-dependent transmissions with different incident angles  $\theta$  for (a)  $\phi=0^\circ$  and  $\Psi=0^\circ$ , and (b)  $\phi=45^\circ$  and  $\Psi=45^\circ$ .

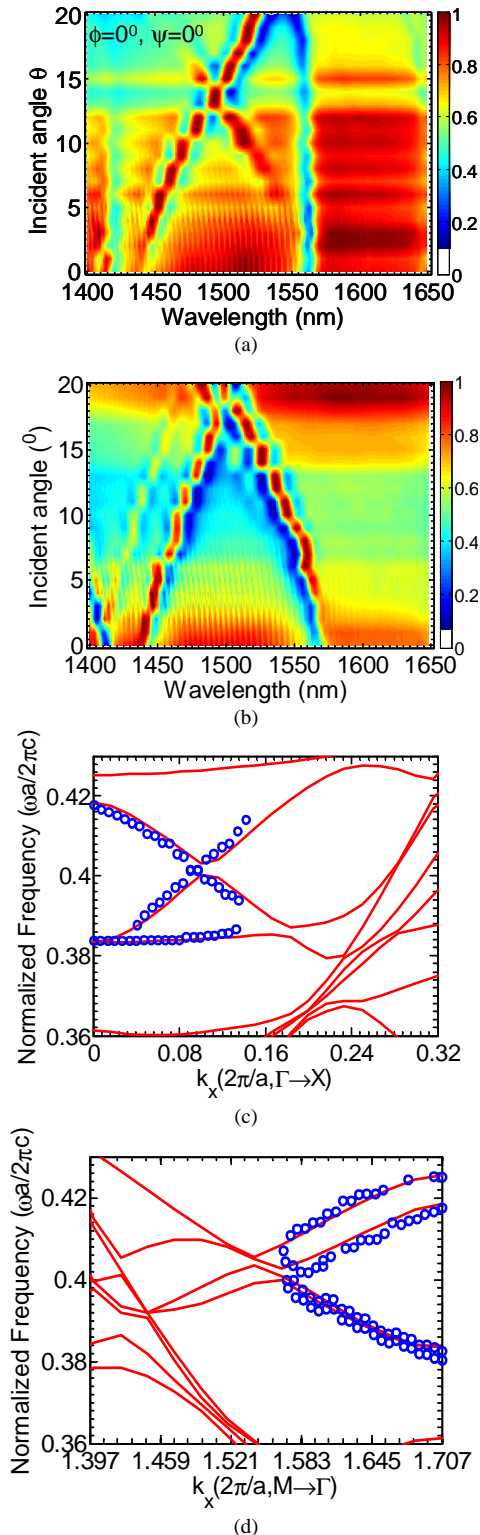


Fig. 5. Measured angle-dependent transmissions with different incident angles  $\theta$  for (a, c)  $\phi=0^0$  and  $\Psi=0^0$ , and (b,d)  $\phi=45^0$  and  $\Psi=45^0$ . In (c, d), measured transmission peaks/dips (circles) agree well with the simulated dispersion curves for different incident angles.

Similar measurements were carried out with  $\phi=45^0$  and  $\Psi=45^0$ , as shown in Fig. 4(b) and Figs. 5(b) and (d). In this

case, when the incident beam varies along  $\Gamma M$  direction, both the modes shift and eventually merge. This also agrees well with the simulated dispersion plot, as shown in Fig. 5(d).

By comparing the spectra of Fig. 4 (a) and (b), it is very clear that our proposed Fano filter is also insensitive to either polarization or sample layout direction under surface normal incidence,  $\theta=0.$ , which is consistent with previous report work with freestanding structure.

## II. CONCLUSIONS

In conclusion, we presented a new Fano filter based on transferred SiNM on PET substrate, which can demonstrate the phenomena of insensitive polarization and angle independence with suitable conditions, in consistent with theoretical work well. Further design and process optimization can lead to higher Q filters, suitable for ultra-compact surface-normal filters, switches, and modulators, for high-density vertical integration of photonic systems and flexible infrared photonics.

## ACKNOWLEDGEMENTS

The authors appreciate the support from NSF, AFOSR, AFRL/CONTACT, and NASA TSGC Programs.

## References

- [1] S. Fan and J. D. Joannopoulos, "Analysis of guided resonances in photonic crystal slabs," *Phys. Rev. B* 65, 235112 (2002).
- [2] Y. Kanamori, T. Kitani, and K. Hane, "Control of guided resonance in a photonic crystal slab using micro-electromechanical actuators," *Appl. Phys. Lett.* 90, 031911 (2007).
- [3] S. A. Scott and M. G. Lagally, "Elastically strain-sharing nanomembranes: flexible and transferable strained silicon and silicon-germanium alloys (Topical Review)," *J. Phys. D: Appl. Phys.* 40, R75-R92 (2007).
- [4] H. C. Yuan, Z. Ma, M. M. Roberts, D. E. Savage, and M. G. Lagally, "High-speed strained-single-crystal-silicon thin-film transistors on flexible polymers," *J. Appl. Phys.* 100, 013708 (2006).
- [5] V. Lousse, W. Suh, O. Kilic, S. Kim, O. Solgaard, and S. Fan, "Angular and polarization properties of a photonic crystal slab mirror," *Opt. Express*, vol. 12, pp. 1575-1582, 2004.